

**A Direct Kinetic Study of the Reaction**  
**K + OH + He → KOH + He by Time-resolved Molecular**  
**Resonance-fluorescence Spectroscopy, OH( $A^2\Sigma^+ - X^2\Pi$ ),**  
**Coupled with Steady Atomic Fluorescence Spectroscopy,**  
**K( $5^2P_J - 4^2S_{1/2}$ )**

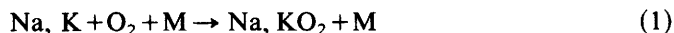
BY DAVID HUSAIN,\* JOHN M. C. PLANE AND CHEN CONG XIANG†

Department of Physical Chemistry, University of Cambridge, Lensfield Road, Cambridge  
 CB2 1EP

*Received 26th March, 1984*

We present the first direct measurement of the absolute rate constant for the third-order reaction  $K + OH + He \rightarrow KOH + He$ . A complex experimental system is described in which a heat-pipe oven, from which atomic potassium is generated, is coupled to a high-temperature reactor for time-resolved resonance-fluorescence measurements on OH following pulsed irradiation. The apparatus is a slow-flow system kinetically equivalent to a static system. Atomic potassium is monitored in the steady mode using resonance fluorescence of the Rydberg transition at  $\lambda = 404$  nm  $K[(5^2P_J) - (4^2S_{1/2})]$  coupled with phase-sensitive detection. Ground-state OH( $X^2\Pi$ ), generated by the repetitively pulsed irradiation of water vapour, is monitored in the time-resolved mode at  $\lambda = 307$  nm  $[OH(A^2\Sigma^+ - X^2\Pi), (0, 0)]$  using molecular resonance-fluorescence measurements following optical excitation with pre-trigger photo-multiplier gating, photon counting and signal averaging. Thus the decay of OH( $X^2\Pi$ ) as a function of time is studied both as a function of  $[K(4^2S_{1/2})]$  and  $[He]$ , yielding the absolute rate constant  $k_3(K + OH + He) = (8.8 \pm 1.8) \times 10^{-31} \text{ cm}^6 \text{ molecule}^{-2} \text{ s}^{-1}$  ( $T = 530$  K). A full account is given of the isolation of this reaction by the use of a 'chemical window' through the control of temperature and the effective elimination of the reaction between  $K_2 + OH$ , and the use of He as the third body which demonstrates negligible collisional quenching efficiency with OH( $A^2\Sigma^+, v' = 0$ ). We also present a detailed extrapolation of the rate data to the environment of flames using unimolecular-reaction-rate theory developed by Tröe and coworkers for dissociation reactions. The agreement between the present results for the isolated reaction extrapolated to flame temperatures and measurements on flames ( $1800 < T/K < 2200$ ), in which  $k_3(K + OH + M)$  (where M stands for the burnt gases of a fuel-rich flame) has been extracted by modelling the complex coupled equilibria, is considered highly satisfactory. Quantitative account of the modelling of the dissociation of KOH is presented in the paper.

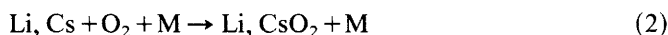
The kinetic study of termolecular reactions of alkali-metal atoms is a subject of renewed experimental interest for both fundamental and applied reasons. It has long been recognised, for example,<sup>1</sup> that many rate data in the literature on reactions of the type



particularly those derived from flame measurements,<sup>2,3</sup> are not in accord with general fundamental considerations of reactions of this type of atomcity by approximately three orders of magnitude.<sup>1</sup> We have subsequently investigated these processes directly for Na and K ( $M = \text{He, N}_2$  and  $\text{CO}_2$ ) by time-resolved atomic resonance

† Permanent address: Department of Modern Chemistry, University of Science and Technology of China, Hefei, Anhui, The People's Republic of China.

absorption spectroscopy following pulsed irradiation of NaI and KI at elevated temperatures.<sup>4,5</sup> The rates of the similar reactions



have been studied by time-resolved multiphoton ionisation spectroscopy of atomic lithium and caesium following pulsed irradiation by Kramer *et al.*<sup>6,7</sup> These recent studies<sup>4-7</sup> have now yielded absolute third-order rate constants for the reactions that are *ca.*  $10^3$  times greater than originally considered.<sup>1</sup> It has subsequently been demonstrated that the previous decay measurements on alkali-metal atoms in oxygen-rich flames<sup>1,2</sup> in fact reflected the variation of chemical equilibria between the alkali-metal atoms, H and OH rather than fundamental rate processes for the alkali-metal atoms.<sup>8,9</sup> Furthermore, absolute rate data for this group of reactions, particularly for Na and K, are used directly in modelling of the alkali-metal atoms in the 90 km region.<sup>10-12</sup> The recent rate measurements<sup>4</sup> on the reactions  $Na + O_2 + M \rightarrow NaO_2 + M$  have considerably improved the agreement between modelling calculations on various forms of sodium in the mesosphere, especially the quantity of sodium bound as  $NaO_2$  and the profile of the cut-off of atomic sodium on the lower side of the 90 km band nearer the earth.<sup>13,14</sup>

The accompanying class of termolecular reactions of alkali-metal atoms in flames which principally control the establishment of the above equilibria includes the processes exemplified by the reaction



which is the object of the present investigation for  $M = He$ . The recombination processes indicated in eqn (3) are routinely employed in equilibrium terms in the flame chemistry of alkali-metal atoms<sup>8,15</sup> and hence the literature in that context is large. In recent years the absolute rate constant for process (3) under flame conditions<sup>16</sup> and the rate constant for the analogous reaction for Na<sup>17</sup> have been determined by Jensen *et al.* from modelling the critical reactions in a flame, namely



This has yielded  $\log_{10}(k_3/\text{cm}^6 \text{ molecule}^{-2} \text{ s}^{-1}) = -(26.8 \pm 0.4) - \log_{10} T$  (in the notation of the paper by Jensen *et al.*<sup>16</sup>) for the burnt gases of a fuel-rich flame ( $N_2 + H_2O + H_2$ ) in the range  $1800 < T/K < 2200$ .<sup>16</sup> The papers of Jensen *et al.*<sup>16,17</sup> may be employed as a modern summary of this general area.

In this paper we describe the first direct measurement of the rate of reaction (3) in which all three reactants are monitored. In contrast to all previous studies of this type of reaction, the third-order process is isolated in real time and the absolute third-order rate constant for  $M = He$  at  $T = 530 \text{ K}$  is reported. Ground-state  $OH(X^2\Pi)$ , generated by the pulsed irradiation of water vapour, is monitored by time-resolved resonance fluorescence of  $OH(A^2\Sigma^+ - X^2\Pi)$  following optical excitation, and atomic potassium in a flow system and derived from a heat-pipe oven is monitored in the steady mode using resonance fluorescence of  $K(5^2P_J - 4^2S_{1/2})$  coupled with phase-sensitive detection. The apparatus is necessarily complex on account of the requirement to monitor two effectively transient species,  $OH(X^2\Pi)$  and  $K(4^2S_{1/2})$ , at elevated temperatures. This type of study may be regarded as analogous to recent investigations of reactions between atoms titrated in a flow-discharge system, such as O, N and H, and a transient molecule such as OH generated by pulsed irradiation, an area reviewed in detail recently by Howard and Smith.<sup>18</sup>

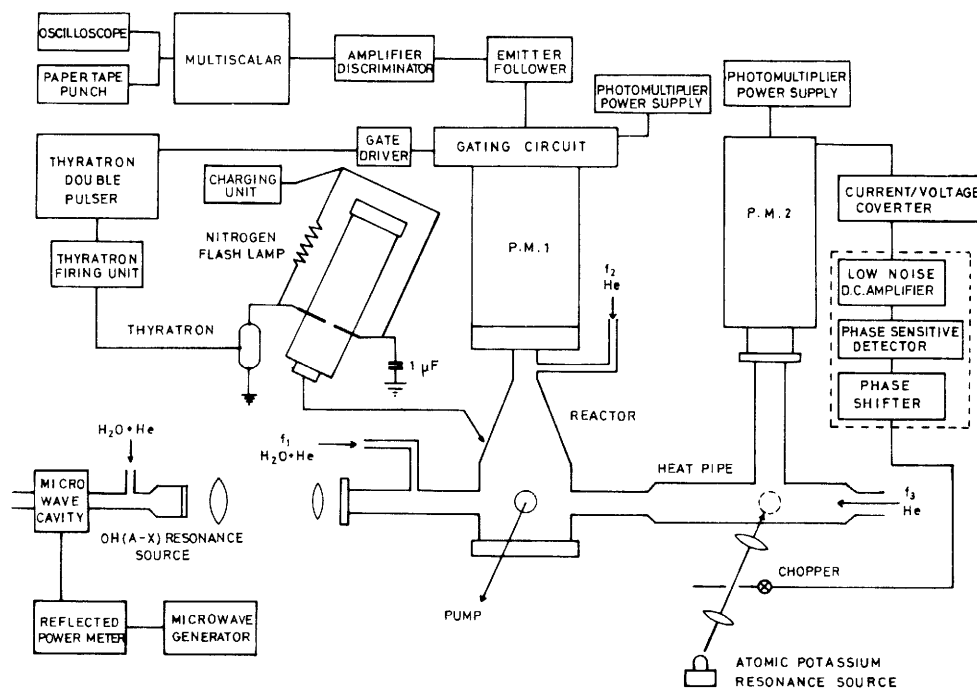


**Fig. 1.** Block diagram of the apparatus for the kinetic study of the reaction  $\text{K} + \text{OH} + \text{M} \rightarrow \text{KOH} + \text{M}$  at elevated temperatures employing (a) time-resolved molecular resonance-fluorescence measurements on  $\text{OH}(X^2\Pi)$  at  $\lambda = 307 \text{ nm}$  [(0, 0),  $\text{OH}[A^2\Sigma - X^2\Pi]$ ] following the pulsed irradiation of  $\text{H}_2\text{O}$  vapour and (b) steady resonance fluorescence coupled with phase-sensitive detection on atomic potassium at  $\lambda = 404 \text{ nm}$  [ $\text{K}(5^2P_J) - \text{K}(4^2S_{1/2})$ ] derived from a heat-pipe oven using a flow system kinetically equivalent to a static system.

Quantitative arguments determining the use of a 'chemical window', (a) by the control of temperature in order to minimise the effect of any reaction between  $\text{K}_2 + \text{OH}$  and (b) by the use of helium as the third body to minimise fluorescence quenching of  $\text{OH}(A^2\Sigma^+)$ ,<sup>19</sup> are presented. The absolute rate constant for reaction (3) with  $\text{M} = \text{He}$ , determined for  $T = 530 \text{ K}$ , is extrapolated to flame temperatures and compositions using unimolecular reaction-rate theory for the reverse process of dissociation following Tröe<sup>20,21</sup> in order to compare the results of the present investigation with the data of Jensen.<sup>16</sup> The resulting agreement is considered to be highly satisfactory.

## EXPERIMENTAL

The block diagram of the apparatus constructed for this study is shown in fig. 1 and is novel. In broad terms atomic potassium, in equilibrium with its liquid at elevated temperatures, is generated in a heat-pipe oven<sup>22</sup> where the relationship between steady atomic resonance fluorescence of  $\text{K}(5^2P_J - 4^2S_{1/2})$  and  $[\text{K}(4^2S_{1/2})]$  is determined for the purpose of empirical calibration. A flow of potassium vapour of known absolute atomic concentration and in the presence of an excess of helium is then subsequently fed to the high-temperature stainless-steel reactor (fig. 1) into which simultaneously flows water vapour in the presence of an excess of helium.  $\text{OH}(X^2\Pi)$  is generated by the pulsed irradiation of the water vapour from a nitrogen-discharge flash lamp<sup>23</sup> (fig. 1) and monitored at elevated temperatures by

time-resolved molecular resonance fluorescence of  $OH(A^2\Sigma^+ - X^2\Pi)$  [ $\lambda = 307$  nm, (0, 0),  $f = 8 \times 10^{-4}$  24] using the photon-counting and signal-averaging procedure described previously.<sup>23,25</sup> The decay of  $OH(X^2\Pi)$  can be described by its removal according to overall third-order rate process (3), together with loss by diffusion, namely

$$-d[OH]/dt = k_{\text{diff}}[OH] + k_3[K][He][OH]. \quad (6)$$

There is an extensive range of kinetic evidence [ref. (23) and references therein] to indicate that such photochemically generated concentrations of  $OH(X^2\Pi)$  are in the region of  $10^{11}$  atom  $\text{cm}^{-3}$ . Concentrations of atomic potassium employed in these measurements are  $> 5 \times 10^{13}$  atom  $\text{cm}^{-3}$  and hence are always in an excess. The overall first-order coefficient for the decay of OH is then given by

$$k' = k_{\text{diff}} + k_3[K][He] \quad (7)$$

and is the object of the present experimental measurements.  $k_{\text{diff}}$  can readily be determined empirically by measurement of the first-order decay of OH in the absence of atomic potassium,<sup>23</sup> and the values we have measured previously<sup>23</sup> for  $k_{\text{diff}}(OH-He)$  are used in the analysis here. This, combined with the determination of  $k'$  for  $OH(X^2\Pi)$  at different values of  $[K(4^2S_{1/2})]$  and  $[He]$ , calculated from the flow calibrations, yields  $k_3$  for the reaction between K, OH and He.

Fig. 2(a) and (b) give a more detailed presentation of the combination of the heat-pipe oven and the high-temperature stainless-steel reactor, and the physical design and coupling to the high-temperature reactor of the  $N_2$  flash discharge lamp used for repetitive pulsing and operating at room temperature. Similarly, the coupling of the photoelectric detection system, also operating at room temperature, to the high-temperature reactor shown in fig. 2. Apart from the major matter of the inclusion and operation of the heat-pipe oven [fig. 2(a)], minor modifications to other components in fig. 2(a) and (b) were necessary, primarily concerning the entry of gas flows and baffle systems in the reactor to ensure mixing of the reactants  $H_2O + K + He$  and to prevent condensation of potassium at appropriate windows. The heat-pipe oven, with cooled side-arms and quartz optical windows attached by means of O-rings [fig. 2(a)] for steady resonance-fluorescence measurements on atomic potassium at  $\lambda = 404$  nm [ $K(5^2P_J) - K(4^2S_{1/2})$ ], was ca. 20 cm in length and of 15 mm internal diameter, and constructed of stainless steel. The operating section of the heat pipe<sup>22</sup> comprised a doubly rolled stainless-steel wick of 120 mesh, 43 gauge, ca. 15 cm in length [fig. 2(a)] with small orthogonally placed apertures for the atomic resonance-fluorescence measurements in the side-arms which also contained wicks. Potassium metal, taken from storage in toluene, was cut into small granules, cleaned in ether in an ultrasonic bath and then quickly inserted into this heat-pipe oven. Solely for the purpose of the purification of the metal this was then run in the heat-pipe-oven mode (see Vidal and Cooper<sup>22</sup>) at 300 °C (573 K) and at a steady pressure of helium of ca. 6 Torr (1 Torr  $\approx 133$  N  $\text{m}^{-1}$ ). Such a high pressure of helium does not, of course, result in a separation of the gas into a pure metal and pure He phase, which would have required pressures of He of only ca. 300 mTorr. This operation of the heat pipe for several hours enables the metal to be thoroughly refluxed and purified. All volatile impurities distilled off into the cooled sections of the heat pipe and were regularly pumped off. During this mode of operation the cooling at  $T_3$  [fig. 2(a)] is switched on to keep the metal vapour phase within the pipe. The progress of the distillation can be monitored using the resonance-fluorescence cell [fig. 2(a)] with chopping of radiation and phase-sensitive detection (E.G.&G. Brookdeal, model 9503-SC) of the steady fluorescence. This was excited by means of a potassium discharge lamp (Phillips Lamp type K 931903) incident through two quartz lenses to focus the light onto the cell, with optical separation by means of a collimator and isolation using an interference filter (Barr and Stroud, type MD 26, band width 18 nm). It was found more convenient to monitor the atomic potassium concentration using the unresolved Rydberg transition at  $\lambda = 404$  nm ( $5^2P_J - 4^2S_{1/2}$ ) rather than the unresolved  $D$  lines at longer wavelength [ $(\lambda = 768$  nm,  $K(4^2P_J - 4^2S_{1/2})$ ]<sup>26</sup> in order to avoid extraneous emission. Photoelectric monitoring of the atomic resonance-fluorescence signal employed an S20 EMI tube (p.m. type 9797B) operating at 750 V. The observed signal is, of course, the complex combination of atomic resonance fluorescence, radiation trapping



and absorption of incident and scattered radiation in the side-arms with varying atomic potassium concentration. An empirical calibration curve relating the signal intensity and  $[K(4^2S_{1/2})]$  was constructed to ensure steady vapour densities during experiments when there was a variable flow through the heat pipe. The concentration of atomic potassium was taken to be the equilibrium vapour pressure above the solid-liquid potassium in the centre of the heat pipe. Since the vapour pressure of  $K(4^2S_{1/2})$  varies particularly rapidly in the temperature range of interest (*ca.*  $10^{-6}$ – $10^{-3}$  atm over the range 427–604 K),<sup>27</sup> accurate calibration of the interior temperature of the heat pipe is necessary. This was achieved by constructing a sliding thermocouple which can be inserted into the reactor through the resonance-lamp coupling and travels the length of the vessel to the end of the heat pipe. The thermocouples  $T_1$ – $T_4$  [fig. 2(a)], which are attached to the outside of the vessel, were accurately calibrated to the temperature inside the vessel. These calibrations were carried out under the normal conditions of an experiment, *i.e.* with the water cooling at  $T_3$  switched off and at a total pressure of He of *ca.* 50 Torr.

When setting up a flow of atomic potassium with He from the heat pipe it was first demonstrated that the measured signal from the K vapour in the heat pipe was unchanged when the cooling at  $T_3$  was switched off, and a flow of He through the heat pipe was varied from 1 to 50 sccm, indicating that the vapour pressure remained at the equilibrium level. The steady-state atomic resonance-fluorescence apparatus (fig. 1) was now transferred to the reactor, with the K spectral lamp incident through the aperture normally used for optical coupling with the OH(A–X) resonance source. The resulting atomic potassium resonance-fluorescence signal could then be used to establish that when the reactor temperature is no lower than 20 K of that of the heat pipe, the metal vapour is not significantly removed by adsorption. Furthermore, when the ratio of the flows  $f_1$ ,  $f_2$  and  $f_3$  is changed (fig. 1) the signal varies qualitatively as expected. To perform this part of the experiment the flows through the inlet pipes on the side arms of the reactor were used [fig. 2(a)]. These are designed according to the system of Fontijn *et al.*<sup>28</sup> to prevent metal being deposited on the cooled windows; approximate calculations of metal diffusion rates at these temperatures and pressures indicated that flows in the side arms of 10–50 sccm of He should prevent this. It was observed during these initial calibration measurements that a reaction appeared to occur between the K vapour and the lamp-black surface of the inside of the reaction vessel, applied to minimise the effect of scattered light,<sup>23</sup> although this reaction quickly ceased, presumably with the formation of intercalation compounds in the carbon, thereafter rendering the surface reasonably inert to K vapour.<sup>29</sup> Thus, following the optical calibrations of atomic potassium both in the heat-pipe oven and in the stainless-steel reactor, together with standard flow calibrations as indicated in previous measurements<sup>23</sup> but which now also include a K + He flow, the flow system was employed as such in the standard manner.

The present time-resolved measurements on OH(A–X) resonance fluorescence employed higher flash energies (50 J) than were used previously,<sup>23</sup> and three flows instead of two. Flow  $f_2$  (fig. 1) was pure He which entered the reactor under the p.m. housing and kept the quartz window beneath the interference filter free of metal. Flow  $f_1$  of  $H_2O + He$  entered the reactor through the two side arms to keep their respective optics free of metal. Flow  $f_3$  carried the metal vapour + He into the reactor where it mixed with the other flows to give a vapour pressure of the metal =  $f_3 / (f_1 + f_2 + f_3) \times$  the pressure of K in the heat pipe. The vapour pressure of water in the reactor that was employed ranged from 100 to 500 mTorr.

The final consideration of the flow system concerns the reaction between atomic potassium and water vapour. According to Jensen *et al.*<sup>16</sup> the reaction between  $K(g)$  and  $H_2O(g)$  is characterised by a rate constant of the form  $\log_{10}(k/cm^3 \text{ molecule}^{-1} \text{ s}^{-1}) = -(9.3 \pm 0.5) - 8700 T^{-1}$ , implying that the rate of this reaction is negligible at the temperature of this system. The reaction between water vapour and liquid potassium on the wick in the heat-pipe oven was avoided by the use of flow  $f_3$  (fig. 1), essentially restricting the water vapour to the volume region of the reactor.

## RESULTS AND DISCUSSION

Fig. 3 shows typical examples of raw data indicating the decay of time-resolved molecular resonance fluorescence due to OH[ $A^2\Sigma^+ - X^2\Pi$ , (0, 0),  $\lambda = 307 \text{ nm}$ ] fol-

lowing the pulsed generation of  $\text{OH}(X^2\Pi)$  in the presence of atomic potassium and the helium third body. The data are in digitised form resulting from the summation of photon counts at  $\lambda = 307$  nm due to optical excitation of OH for a large number of individual experiments. We have demonstrated previously<sup>23,25</sup> that the resonance fluorescence due to  $\text{OH}(A-X)$  is given by

$$I_F(t) = \frac{\phi[\text{OH}(X^2\Pi)_{t=0}] \exp(-k't)}{1 + \sum k_Q[Q]/A_{nm}} \quad (\text{i})$$

where the symbols have their usual significance<sup>23,25</sup> and the term  $\sum k_Q[Q]$  represents an average contribution to the collisional quenching of  $\text{OH}(A^2\Sigma^+, v'=0)$  in the various rotational states. Some further consideration of this fluorescence-quenching term is necessary here because of its particular effect on the 'chemical window' (see introduction) and, in this context, on limitations on the choice of third body in reaction (3) to helium for the present type of investigation. The essential independence of fluorescence quenching of  $\text{OH}(A^2\Sigma^+)$  by  $\text{H}_2\text{O}$  with temperature<sup>19,30</sup> coupled with the use of  $A_{nm}[\text{OH}(A^2\Sigma^+-X^2\Pi), (0,0)] = \text{ca. } 1.4 \times 10^6 \text{ s}^{-1}$ ,<sup>24</sup> indicates typical values of  $k_Q[Q]/A_{nm} \approx 3$  for the present experiments. Thus apart from limitations arising from light collection in the photoelectric detection optics, only 25% of the optically excited  $\text{OH}(A^2\Sigma^+)$  fluoresces, excluding any fluorescence quenching of  $\text{OH}(A^2\Sigma^+)$  by atomic potassium. Fortunately, fluorescence quenching of  $\text{OH}(A^2\Sigma^+)$  by He is negligible.<sup>31</sup> Unfortunately, that for  $\text{N}_2$ , for example, is not  $\{k[\text{OH}(A^2\Sigma^+) + \text{N}_2] = 2.2^{+1.8}_{-1.2} \times 10^{-11} \text{ cm}^3 \text{ molecule}^{-1} \text{ s}^{-1}, T = 300 \text{ K}\}$ .<sup>31</sup> Thus, for conditions of the type indicated in fig. 3 with  $\text{N}_2$  replacing He as the third body, a typical value of  $\sum k_Q[Q]/A_{nm}$  would be ca. 8 for even a low concentration of  $\text{N}_2 \approx 2 \times 10^{17} \text{ molecule cm}^{-3}$ . Thus no  $\text{OH}(A-X)$  resonance-fluorescence signals could be detected with  $\text{N}_2$  as the third body, as expected.

The full curves in fig. 3 represent computerised curve-fitting of the digitised data to the now standard form:

$$I_F(t) = \theta_1 + \theta_2 \exp(-k't) \quad (\text{ii})$$

using the LAMFIT procedure of Powell<sup>32</sup> as previously employed,<sup>23,25</sup> where  $\theta_1$  describes the steady scattered light component and the second term in eqn (ii), the right-hand side of eqn (i). The general magnitude of  $\theta_1$  is indicated visually by the 'long-time' values of  $I_F$  (fig. 3) and its actual magnitude is computed for each decay trace. Pseudo-first-order plots constructed from the data of fig. 3 using these values of  $\theta_1$   $\{\ln [I_F(t) - \theta_1]$  against  $t\}$  are shown in fig. 4 for the purpose of visual display of first-order kinetics due to  $\text{OH}(X^2\Pi)$ . Plots of the type given in fig. 4 demonstrate the scatter automatically generated with the direct use of a logarithmic variation. All values of  $k'$  presented here were, in fact, derived from direct curve fitting as indicated in fig. 3.

Fig. 5 shows the variation of  $k'$  for the decay of  $\text{OH}(X^2\Pi)$  with the concentration of atomic potassium, indicating the first-order kinetics of the latter. These are presented for different concentrations of atomic helium. Fig. 6 shows the diffusion-corrected second-order decay coefficients for the removal of  $\text{OH}(X^2\Pi)$  in the presence of effectively constant atomic potassium concentrations with varying concentrations of atomic helium, indicating the first-order kinetic behaviour of the latter. All the rate data from the present investigation are combined by rearranging eqn (7) in the form

$$(k' - k_{\text{diff}})/[\text{He}] = k_3[\text{K}] \quad (\text{8})$$

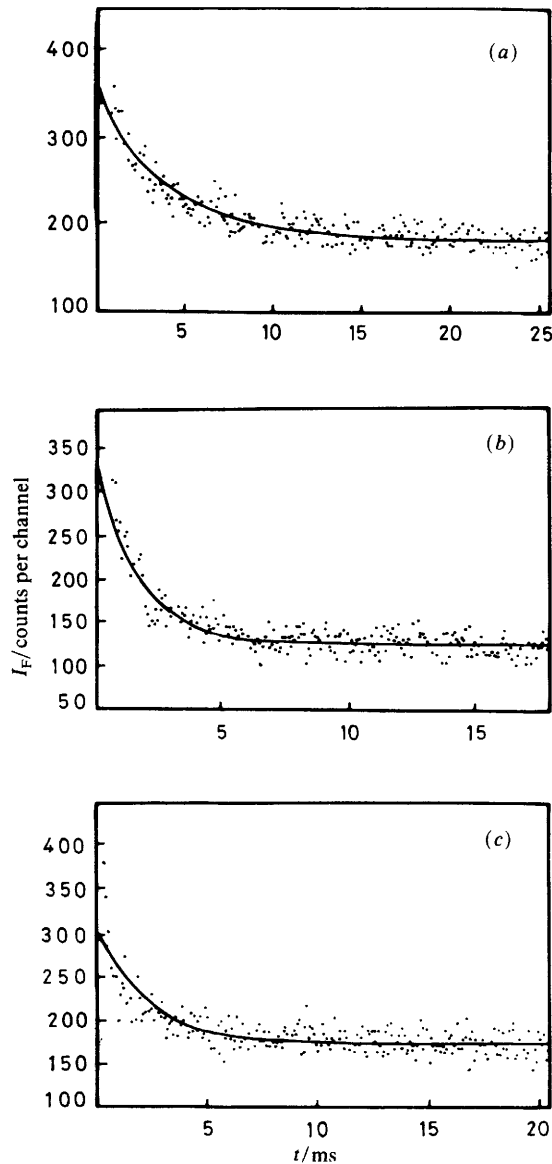


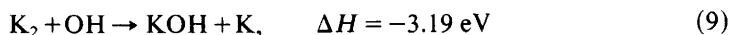
**Fig. 3.** Digitised time-variation of the light intensity at  $\lambda = 307$  nm indicating the decay of time-resolved molecular resonance fluorescence due to OH [ $I_F$ /counts per channel, (0, 0), OH( $A^2\Sigma^+ - X^2\Pi$ )] following the pulsed irradiation of  $\text{H}_2\text{O}$  vapour in the presence of atomic potassium derived from a heat-pipe oven and monitored in the steady mode using atomic resonance fluorescence at  $\lambda = 404$  nm [ $\text{K}(5^2P_J) - \text{K}(4^2S_{1/2})$ ] coupled with phase-sensitive detection.  $T = 530$  K,  $E = 50$  J, repetition rate = 1 Hz, no. of individual experiments = 256, (—) computerised fit to the form  $I_F = \theta_1 + \theta_e \exp(-k't)$ .

	[K]/ $10^{13}$ atom $\text{cm}^{-3}$	[He]/ $10^{17}$ atom $\text{cm}^{-3}$
(a)	6.6	8.7
(b)	53	8.7
(c)	50	3.8

and are presented graphically in this form in fig. 7. The slope of this plot yields

$$k_3(\text{K} + \text{OH} + \text{He}) = 8.8 \pm 1.8 \times 10^{-31} \text{ cm}^6 \text{ molecule}^{-2} \text{ s}^{-1} \quad (T = 530 \text{ K}).$$

The quoted error includes both the  $2\sigma$  error arising from fig. 7 and the uncertainty in the vapour pressure of potassium (*ca.* 15%) resulting from the uncertainty in the temperature measurement ( $\pm 5^\circ\text{C}$ ) in the heat-pipe oven. This result for  $k_3$  constitutes the first direct measurement not only of this particular reaction for any third body M, but for any reaction of the type  $\text{X} + \text{OH} + \text{M} \rightarrow \text{XOH} + \text{M}$  for a metal X. Before proceeding with the discussion of this result and, in particular, the extrapolation to high temperatures using unimolecular-reaction-rate theory,<sup>20,21</sup> the final aspect of the 'chemical window' restricting measurement of  $k_3$  to temperatures of the magnitude employed here is considered. In approximate terms  $k_3$  is expected to vary roughly with the form  $T^{-1}$ .<sup>15</sup> The extrapolation procedure (see later) will be concerned with relatively small departures from this type of temperature dependence which will have a major effect on rates predicted from flame temperatures. However, for the present experimental considerations with this system use of this simple temperature dependence is adequate. First, the lowest temperature conveniently employed is determined by the use of  $[\text{K}(4^2\text{S}_{1/2})]$ , which will be sensibly in excess of  $[\text{OH}(X^2\Pi)]$  generated on photolysis. Secondly, one factor governing the upper temperature limit that can be employed is the apparatus itself, where the use of a copper gasket [fig. 2(a)] restricts temperatures to  $T < ca. 700 \text{ K}$ . More important are kinetic considerations. A temperature dependence of the form  $T^{-1}$  will barely be detected *via* the measured rate constant  $k_3$  across a temperature range of *ca.* 530–700 K. The principal consideration, however, concerns the role of the highly exothermic reaction



$\{D_0^\circ[\text{K}_2(X^1\Sigma_g^+)] = 0.514 \text{ eV}, D_0^\circ(\text{K}-\text{OH}) = 3.71 \text{ eV}\}^{27,33}$  which we may estimate as proceeding at a rate close to the collision number, say,  $10^{-10} \text{ cm}^3 \text{ molecule}^{-1} \text{ s}^{-1}$ . For the present experiments we may calculate the equilibrium constant for the reaction



as  $K_{\text{eq}}(T = 530 \text{ K}) = 1.46 \times 10^{-18} \text{ cm}^{-3} \text{ molecule}^{-1}$ .<sup>27</sup> This implies that for the maximum concentration of  $\text{K}(4^2\text{S}_{1/2})$  employed here of *ca.*  $6 \times 10^{14} \text{ atom cm}^{-3}$  the maximum contribution to the first-order decay coefficient for the removal of  $\text{OH}(X^2\Pi)$  by rate process (9) will be *ca.*  $50 \text{ s}^{-1}$  and is generally negligible when compared with the natural scatter in the measurements. Thus the present experimental conditions isolate reaction (3). However, whilst raising the temperature displaces the above equilibrium from right to left, the absolute value of  $[\text{K}_2]$  nevertheless increases, as seen from the vapour-pressure data,<sup>27</sup> and so will the magnitude of  $k_3[\text{K}_2]$ . This first-order coefficient will not only be large but will increase the overall observed decay rate for  $\text{OH}(X^2\Pi)$  as a function of increasing temperature much more rapidly than the decrease in  $k_3$ , which would not be detected nor, indeed, measured by difference.

#### EXTRAPOLATION OF $k_3(\text{K} + \text{OH} + \text{He})$ TO HIGH TEMPERATURES AND COMPARISON WITH MEASUREMENTS DERIVED FROM FLAMES

The absolute determination of  $k_3$  described here by direct measurements on  $\text{OH}(X^2\Pi)$ ,  $\text{K}(4^2\text{S}_{1/2})$  and He is of fundamental interest and may be considered in

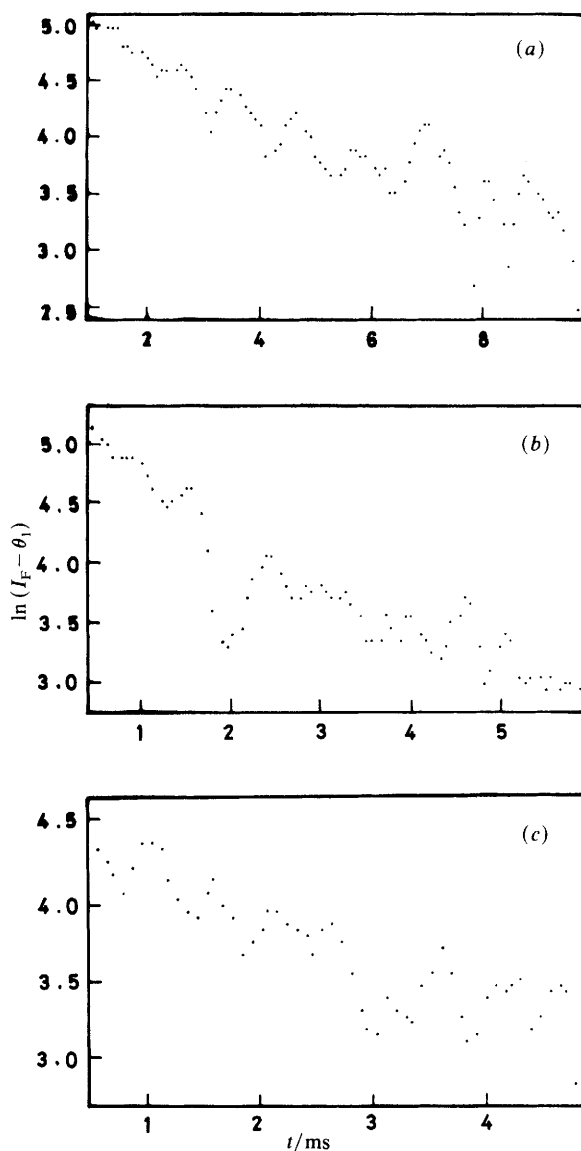


**Fig. 4.** Pseudo-first-order plots  $[\ln(I_F - \theta_1)]$  against  $t$  of the fluorescence intensity at  $\lambda = 307$  nm indicating the decay of time-resolved molecular resonance fluorescence due to OH  $[(0, 0), \text{OH}(A^2\Sigma^+ - X^2\Pi)]$  following the pulsed irradiation of  $\text{H}_2\text{O}$  vapour in the presence of atomic potassium derived from a heat-pipe oven and monitored in the steady mode using atomic resonance fluorescence at  $\lambda = 404$  nm  $[\text{K}(5^2P_J) - \text{K}(4^2S_{1/2})]$  coupled with phase-sensitive detection.  $T = 530$  K,  $E = 50$  J, repetition rate = 1 Hz, no. of individual experiments = 256.

	$[\text{K}]/10^{13} \text{ atom cm}^{-3}$	$[\text{He}]/10^{17} \text{ atom cm}^{-3}$
(a)	6.6	8.7
(b)	53	8.7
(c)	50	3.8

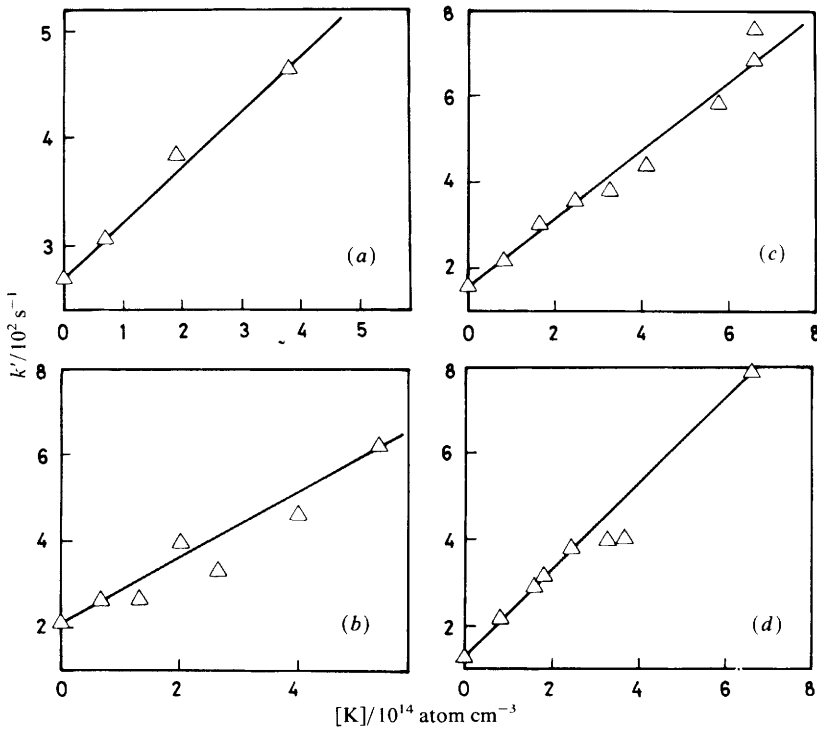


**Fig. 5.** Variation of the pseudo-first-order rate coefficient,  $k'$ , for the decay of OH obtained by time-resolved molecular resonance-fluorescence measurements on OH( $X^2\Pi$ ) [ $\lambda = 307$  nm, (0, 0), OH( $A^2\Sigma-X^2\Pi$ )] following the pulsed irradiation of H<sub>2</sub>O vapour in the presence of different concentrations of atomic potassium, monitored in the steady mode using atomic fluorescence of the resonance transition at  $\lambda = 404$  nm [ $K(5^2P_j)-K(4^2S_{1/2})$ ] coupled with phase-sensitive detection ( $T = 530$  K). [He]/10<sup>17</sup> atom cm<sup>-3</sup>: (a) 5.85, (b) 8.71, (c) 10.0 and (d) 12.4.

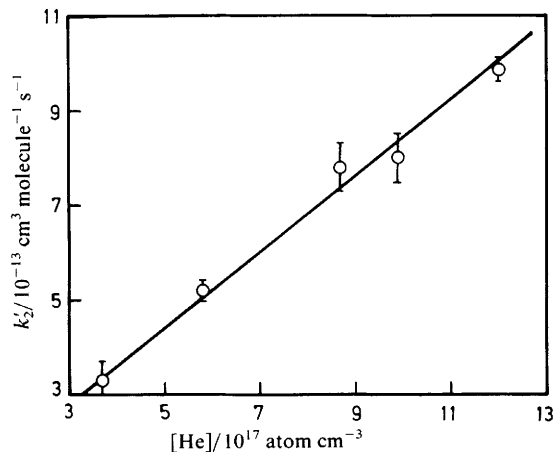


**Fig. 6.** Variation of the pseudo-second-order rate coefficient,  $k_2'$  ( $=k'/[K(4^2S_{1/2})]$ ), for the decay of OH as a function of the atomic helium concentration obtained by time-resolved molecular resonance-fluorescence measurements on OH( $X^2\Pi$ ) [ $\lambda = 307$  nm, (0, 0), OH( $A^2\Sigma^+-X^2\Pi$ )] following the pulsed irradiation of H<sub>2</sub>O vapour, with monitoring of atomic potassium by steady resonance fluorescence at  $\lambda = 404$  nm [ $K(5^2P_j)-K(4^2S_{1/2})$ ] coupled with phase-sensitive detection ( $T = 530$  K).

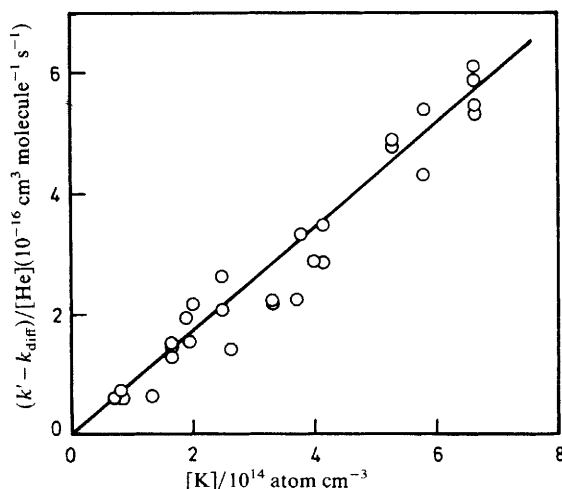


**Fig. 7.** Variation of the diffusion-corrected pseudo-second-order rate coefficient,  $(k' - k_{\text{diff}})/[\text{He}]$ , for the decay of OH as a function of the atomic potassium concentration, obtained by time-resolved molecular resonance-fluorescence measurements on OH( $X^2\Pi$ ) [ $\lambda = 307$  nm, (0, 0), OH( $A^2\Sigma^+ - X^2\Pi$ )] following the pulsed irradiation of  $\text{H}_2\text{O}$  vapour, with monitoring of atomic potassium by steady resonance fluorescence at  $\lambda = 404$  nm [ $\text{K}(5^2P) - \text{K}(4^2S_{1/2})$ ] coupled with phase-sensitive detection ( $T = 530$  K).

the broader context of atom–molecule recombination reactions<sup>18</sup> and in its application to modelling of flames. For experimental reasons that have been given, the present type of measurement is restricted to a single-temperature investigation and to a third body causing no significant fluorescence quenching of OH( $A^2\Sigma^+$ ,  $v' = 0$ ), namely, He. Thus, comparison with data derived from flames<sup>17</sup> requires an extrapolation of  $k_3$  over a wide range of temperature that is more detailed than that of the simplified approach using a  $T^{-1}$  dependence necessarily employed for a large body of recombination-rate data considered by Jensen and Jones.<sup>15</sup> Further, the extrapolation must include the effects of different intermolecular interactions for various third bodies in process (3), in the present case for He and the bulk materials in the burnt gases of a fuel-rich flame, namely,  $\text{H}_2 + \text{N}_2 + \text{H}_2\text{O}$ .<sup>15</sup> In turn, this affects the temperature dependence of  $k_3$ , an important aspect in view of the wide temperature range over which the extrapolation is carried out. The extrapolation is performed not only to make a quantitative comparison of the present measurements on  $k_3$  with those from flames, but also as a quantitative test of the modelling procedure used to extract fundamental rate data from the set of equilibrium processes that have to be included in the analysis of the complex medium of a flame.

We employ the procedure of Tröe<sup>20,21</sup> using simplified equations based on R.R.K.M. theory,<sup>20,21</sup> yielding the quantitative estimation of the second-order rate constant for the reverse unimolecular decomposition in the low-pressure limit and hence used to calculate the rate constant for the third-order association reaction *via* the equilibrium constant, an overall approach recommended recently by the NASA review panel for third-order rate constants.<sup>34</sup> Thus, following Tröe,<sup>20</sup> the rate constant of a thermal unimolecular reaction in the limiting low-pressure range ( $k_0$ ) is expressed as a product of a strong-collision rate constant  $k_0^{\text{sc}}$  and a weak-collision efficiency,  $\beta_c$ , for the energy transfer:

$$k_0 = \beta_c k_0^{\text{sc}}. \quad (a)$$

Following solution of the R.R.K.M. master equation, a simple expression for the collisional efficiency,  $\beta_c$ , is derived in terms of the average energy transferred per collision (see below). The strong-collision rate constant may be expressed in the standard form<sup>21</sup>

$$k_0^{sc} = \frac{Z_{LJ}\rho(E_0)RT \exp(-E_0/RT)}{Q_{vib}} F_E F_{anh} F_{rot} F_{rot,int} F_{corr} \quad (b)$$

where  $Z_{LJ}$  is the Lennard-Jones reference collision frequency and  $\rho(E_0)$  is the density of states at the critical energy  $E_0$ ;  $F_E$ ,  $F_{anh}$ ,  $F_{rot}$  and  $F_{rot,int}$  are the correction terms for the energy dependence of the density of states arising from the energy  $E$ , anharmonicity, rotation and internal rotation, respectively.  $F_{corr}$  is a correction factor to account for coupling between different degrees of freedom and is usually taken as unity.  $Q_{vib}$  is the vibrational partition function.  $Z_{LJ}$  is calculated in the standard manner<sup>21</sup> in terms of the appropriate collision integrals<sup>35</sup> and the Lennard-Jones parameters are estimated by means of the usual combining rules.<sup>35</sup> Particular consideration in the present calculation must be given to the total number of oscillators,  $s$ , and the differences in the number of oscillators in the reactant and product molecules,  $m$ <sup>20,21</sup> (see later).

The barrier to association for the reaction  $K + OH + M$  is likely to be a small centrifugal one,<sup>36</sup> which is neglected here so that the critical energy  $E_0$  may be identified with  $\Delta H_0^\circ$ , the enthalpy change for the reaction at 0 K. The association rate constant,  $k_{rec,0}^{sc}$  may be obtained from  $k_0^{sc}$  via the equilibrium constant,  $K_{eq}$ :

$$k_{rec,0}^{sc} = K_{eq} k_0^{sc} \quad (c)$$

$k_{rec,0}^{sc}$  represents an upper limit for the rate constant and must be multiplied by the collision deactivation efficiency  $\beta_c$  ( $0 < \beta_c < 1$ ) to obtain a value than can be compared with experiment. The temperature dependence of  $\beta_c$  is given by

$$\frac{\beta_c}{1 - \beta_c^{1/2}} = \frac{\langle \Delta E \rangle}{F_E RT} \quad (d)$$

where  $\langle \Delta E \rangle$  is the average energy transferred per collision; comparison with experimental data at one temperature enables  $\langle \Delta E \rangle$  to be calculated.  $\langle \Delta E \rangle$  is usually assumed to be independent of temperature, or, in the case of helium as a third body, proportional to  $T^{1/2}$ .<sup>37,38</sup>  $k_0^{sc}$  and  $\beta_c$  may then be calculated at a different temperature,  $k_0$  estimated together with  $K_{eq}$ , and thus an estimate of  $k_{rec,0}$  can be made.

The rate data for reactions of the type (3) reported by Jensen *et al.*<sup>16</sup> were derived from measurements on the depletion of atomic potassium in the burnt gases of a fuel-rich flame ( $H_2 + N_2 + H_2O$ ) assuming KOH is the only compound of potassium produced to any significant extent and employing the pair of equilibria (4) and (5). This yielded<sup>16</sup>  $\log_{10}(k_3/\text{cm}^6 \text{ molecule}^{-2} \text{ s}^{-1}) = -(26.8 \pm 0.4) - \log_{10} T$ . This gives a central value of  $k_3 = 7.7 \times 10^{-31} \text{ cm}^6 \text{ molecule}^{-2} \text{ s}^{-1}$  at a temperature of 2055 K at which most of the flame measurements were carried out, with a wide range in the upper and lower bounds  $(3.1 \text{ to } 19.4) \times 10^{-31} \text{ cm}^6 \text{ molecule}^{-2} \text{ s}^{-1}$ . In order to compare the present result for  $k_3$  ( $M = \text{He}$ ) with the flame data, we follow the further procedure of Trøe *et al.*,<sup>37,39</sup> who have shown that since all terms in eqn (b) other than  $Z_{LJ}$  are independent of the third body,  $M$ , the collision efficiency,  $\beta_M$  of any third-body,  $M$ , relative to that of He, say, can be written as

$$\frac{\beta_M}{\beta_{He}} = \frac{k_M Z_{LJ}(M)}{k_{He} Z_{LJ}(He)} \quad (e)$$

Furthermore, there is a variety of evidence<sup>37</sup> to indicate that these efficiencies at a given temperature are approximately independent of the nature of the reaction. Thus, we may employ the results of rate data derived from high temperature measurements on unimolecular dissociation reactions in shock tubes<sup>37,40</sup> yielding  $\beta_{\text{N}_2}/\beta_{\text{He}} = ca. 0.5$  at 2000 K. Since water does not appear to have been studied explicitly as a third body at high temperature, an approximate value for  $\beta_{\text{H}_2\text{O}}/\beta_{\text{He}} = 3.3\text{--}4.2$  is obtained by noting that for the reactions  $\text{H} + \text{O}_2 + \text{M}$  and  $\text{OH} + \text{NO} + \text{M}$ , where  $\text{M} = \text{H}_2\text{O}$ , at room temperature<sup>34</sup>  $\beta_{\text{H}_2\text{O}}/\beta_{\text{N}_2} = ca. 6.5$  and by assuming that this ratio does not change by  $>30\%$  over the range in temperature to 2000 K. [See ref (37), which lists the relative efficiencies over such a temperature range of other efficient quenching gases such as  $\text{CO}_2$  and  $\text{SF}_6$ .]

The after-burning region of the flames studied by Jensen *et al.*<sup>16</sup> consisted of 25%  $\text{H}_2\text{O}$  and 75% ( $\text{H}_2$  or  $\text{N}_2$ ). The assumption of equivalent collision efficiencies for  $\text{H}_2$  and  $\text{N}_2$ , and using data from table 1 (see later) to evaluate the relevant collision frequencies between the third bodies and the initially formed  $\text{KOH}$ , indicates that  $k_{\text{flame}}/k_{\text{He}} = 1.2\text{--}1.7$ . Thus we may modify Jensen's data<sup>16</sup> for  $\text{M} = \text{He}$  to yield  $k_3(\text{K} + \text{OH} + \text{He}, 2055 \text{ K}) = 1.8 \times 10^{-31} \text{ cm}^6 \text{ molecule}^{-2} \text{ s}^{-1}$  for the lowest estimate, with a best estimate of  $5.1 \times 10^{-31} \text{ cm}^6 \text{ molecule}^{-2} \text{ s}^{-1}$ . Alternatively, the present value for  $k_3(\text{K} + \text{OH} + \text{He})$  may be adjusted for  $\text{M} = \text{flame medium}$ . Assuming that  $\beta_{\text{N}_2}$  or  $\beta_{\text{H}_2}/\beta_{\text{He}} \approx 2$  and  $\beta_{\text{H}_2\text{O}}/\beta_{\text{He}} \approx 13$  at  $T = 530 \text{ K}$ , this yields  $k_3[\text{K} + \text{OH} + \text{M}(\text{flame medium}), T = 530 \text{ K}] = 4.1 \times 10^{-30} \text{ cm}^6 \text{ molecule}^{-2} \text{ s}^{-1}$ .

#### DATA INPUT FOR CALCULATIONS

##### LENNARD-JONES PARAMETERS

The Lennard-Jones model is not a good description of the intermolecular forces involving a highly polar molecule such as  $\text{KOH}$  ( $\mu = 8.5 \text{ D}$ ).<sup>41</sup> Even variations such as the Stockmayer potential have not been used for molecules with a dipole moment above *ca.* 2.5 D.<sup>35</sup> On the other hand, the attractive forces between  $\text{He}$  and  $\text{KOH}$  will not be nearly so great, and the Lennard-Jones collision frequency advocated in the Tröe formalism<sup>21</sup> is a useful reference frequency in this case. We have therefore estimated  $\sigma$  and  $\epsilon/k$  for  $\text{KOH}$  using the relations<sup>42</sup>

$$\sigma/\text{\AA} = (1.58 V_b)^{1/3} \quad (f)$$

$$(\epsilon/k)/\text{K} = (1.18 T_b) \quad (g)$$

where  $V_b$  and  $T_b$  are the molar volume and temperature at the boiling point ( $1 \text{ \AA} = 0.1 \text{ nm}$ ). This yields  $\sigma_{\text{KOH}} = 4.07 \text{ \AA}$  and  $\epsilon_{\text{KOH}}/k = 1880 \text{ K}$  using  $T_b = 1595 \text{ K}$ ,<sup>43</sup> and estimating  $V_b$  from density measurements of the molten salt.<sup>44</sup>  $\sigma_{\text{KOH}+\text{He}}$  and  $\epsilon_{\text{KOH}+\text{He}}/k$  are then obtained using the usual combining rules.<sup>35</sup> In fact, it can be demonstrated that whilst the actual values of  $\sigma_{\text{KOH}+\text{He}}$  and  $\epsilon_{\text{KOH}+\text{He}}/k$  that are used to calculate  $Z_{\text{LJ}}$  do have some effect on the value of  $\beta_c$  and  $\langle \Delta E \rangle$  that are obtained, they have little influence on the temperature extrapolation and the value of  $n$  (see later) that is finally obtained in the calculation.

##### FUNDAMENTAL FREQUENCIES AND DISSOCIATION ENERGY OF $\text{KOH}$

Recent measurements<sup>41,43</sup> indicate that  $\text{KOH}$  in the gas phase is a linear molecule with a  $\text{KO}$  bond length of  $2.18 \text{ \AA}$  and an  $\text{O-H}$  bond length of  $0.97 \text{ \AA}$ . The  $\text{KO}$  stretching frequency has been measured from microwave spectroscopy<sup>45</sup> as  $390 \pm 40 \text{ cm}^{-1}$ , the degenerate bending modes have been estimated as  $320 \pm 30 \text{ cm}^{-1}$ ,<sup>16</sup> confirming earlier work of Jensen,<sup>46</sup> and the  $\text{OH}$  stretch as  $3660 \text{ cm}^{-1}$ .<sup>44</sup> The  $\text{OH}$

bond length and frequency are similar to the theoretical predictions for  $\text{OH}^-$ .<sup>41</sup> Indeed, SCF calculations on linear KOH by England<sup>41</sup> show that the Mulliken electron populations in the region of the minimum of the potential well are 18.1 electrons associated with the K atom, 9.4 electrons associated with the O atom and 0.5 electrons with the H atom, closely corresponding to the structure  $\text{K}^+(\text{OH})^-$ . The bond energy of the KO bond in KOH is taken as  $D_0 = 357.3 \pm 1.2 \text{ kJ mol}^{-1}$  from the 1974 supplement to the JANAF Tables.<sup>43</sup> The same source is used for the relevant information on OH required for calculation of the equilibrium constant,  $K_{\text{eq}}$ .

#### APPLICATION OF THE TRÖE FORMALISM

In order to estimate the strong-collision dissociation rate constant for KOH, account should first be taken of the nature of the potential surface over which dissociation will occur. England<sup>41</sup> has calculated self-consistent field, multiconfigurational self-consistent field and MC followed by configuration-interaction potential-energy curves for the linear-path dissociation of KOH to  $\text{K} + \text{OH}$ . He shows that KOH is highly ionised, giving rise to a very slowly varying function of the KO bond length near the minimum geometry, typical of highly ionic compounds and in agreement with the experimental value of  $408 \text{ cm}^{-1}$  for the stretching frequency of the KO bond in KOH.<sup>46</sup>

Following the methods of Grice and Herschbach<sup>36</sup> (and assuming KOH to be analogous to its isoelectronic counterpart KF), the avoided crossing between the diabatic ionic and covalent curves of KOH occurs at a KO bond length of  $5.9 \text{ \AA}$ . The resulting adiabatic curves from the mixing of the ionic and covalent states will have a splitting at this KO distance of *ca.*  $34 \text{ kJ mol}^{-1}$ , and thus curve crossing should not play a part in the dissociation process: according to the Landau-Zener formula, for example, the probability is essentially zero.<sup>47</sup> There are not likely to be any barriers to dissociation and there will be a small centrifugal barrier to association. This barrier can be estimated by assuming a modified attractive van der Waals-type potential in the forming bond,<sup>21</sup> using  $C^* = 2E_0/r_c^6$  and  $V(r) = C^*/r^6$ , where  $r_c$  is the equilibrium bond length and  $r$  is the length of the breaking bond. At the thermal temperatures in the present system, the maximum impact parameter  $b^* \approx 6.56 \text{ \AA}$ , corresponding to a centrifugal barrier for the recombination of  $6.52 \text{ kJ mol}^{-1}$ .<sup>47</sup> This situation corresponds to the case-II potential considered by Tröe.<sup>21</sup>

The present calculations are carried out using two models of KOH, A and B. In model A the Tröe formalism is applied with  $s = 4$  and  $m = 3$ , *i.e.* the molecule is considered to have four oscillators, three of which are described as Morse potentials and the OH vibration which is considered to be harmonic. Model B takes into account the potential function of ionic KOH slowly varying with  $r$ , owing to attractive  $1/r$  Coulombic forces, so that dissociation to the covalent products is only achieved at KO bond lengths  $> 5.9 \text{ \AA}$ . Also, the very low bending frequency of vibration of KOH is approximated to be  $320 \pm 30 \text{ cm}^{-1}$ .<sup>45</sup> This model implies that in molecules of KOH, which are highly vibrationally excited with energies close to  $E_0$ , these degenerate bending modes will be transformed into two free rotors, *i.e.*  $s = 2$ ,  $m = 1$  and  $r = 2$ , the number of free rotors. Johnston<sup>48</sup> considers a similar transformation in the dissociation of NOCl.

The results of the calculations employing both of these models are shown in table 1. The collision efficiencies,  $\beta_c$ , for He as a bath gas are estimated by comparison with the value at 530 K from the present work. Model A gives a value of  $\beta_c$  at 530 K of 0.05 which is particularly low and difficult to interpret in terms

**Table 1.** Extrapolation of rate data for the reaction  $\text{K} + \text{OH} + \text{He} \rightarrow \text{KOH} + \text{He}$ Data for  $\text{K} + \text{OH} + \text{He}$  at  $T = 530 \text{ K}$ 

$$\sigma_{\text{LJ}} = 3.32 \text{ \AA} \quad \epsilon_{\text{LJ}}/k = 138.6 \text{ K}$$

$$Z_{\text{LJ}} = 6.21 \times 10^{-10} \text{ cm}^3 \text{ molecule}^{-1} \text{ s}^{-1}$$

$$E_0 = 357.3 \text{ kJ mol}^{-1} \quad E_z = 27.9 \text{ kJ mol}^{-1}$$

$$K_{\text{eq}} = 1.23 \times 10^{11} \text{ cm}^3 \text{ molecule}^{-1}$$

model A

$$s = 4 \quad m = 3 \quad r = 0$$

$$v_1 = 408 \text{ cm}^{-1} \quad v_2 = v_3 = 340 \text{ cm}^{-1} \quad v_4 = 3660 \text{ cm}^{-1}$$

$$Q_{\text{vib}} = 4.162 \quad a = 0.9765 \quad \rho(E_0) = 2.795$$

$$F_E = 1.034 \quad F_{\text{anh}} = 1.728 \quad F_{\text{rot}} = 6.740$$

$$k_0^{\text{sc}} = 1.35 \times 10^{-40} \text{ cm}^3 \text{ molecule}^{-1} \text{ s}^{-1}$$

$$k_{\text{rec},0}^{\text{sc}} = 1.66 \times 10^{-29} \text{ cm}^6 \text{ molecule}^{-2} \text{ s}^{-1}$$

$$\beta_c = 0.053 \quad \langle \Delta E \rangle = 314 \text{ J mol}^{-1}$$

model B

$$s = 2 \quad m = 1 \quad r = 2$$

$$v_1 = 408 \text{ cm}^{-1} \quad v_2 = 3660 \text{ cm}^{-1}$$

$$Q_{\text{vib}} = 1.500 \quad a = 0.9832 \quad \rho(E_0) = 0.00185$$

$$F_E = 1.011 \quad F_{\text{anh}} = 2 \quad F_{\text{rot}} = 7.818$$

$$F_{\text{rot.int}}^{\text{free}} = 43.656$$

$$k_0^{\text{sc}} = 1.42 \times 10^{-41} \text{ cm}^3 \text{ molecule}^{-1} \text{ s}^{-1}$$

$$k_{\text{rec},0}^{\text{sc}} = 1.75 \times 10^{-30} \text{ cm}^6 \text{ molecule}^{-2} \text{ s}^{-1}$$

$$\beta_c = 0.50 \quad \langle \Delta E \rangle = 7700 \text{ J mol}^{-1}$$

Data for  $\text{K} + \text{OH} + \text{He}$  at  $T = 2055 \text{ K}$ 

$$K_{\text{eq}} = 2.65 \times 10^{-15} \text{ cm}^3 \text{ molecule}^{-1}$$

model A

$$k_{\text{rec},0}^{\text{sc}} = 5.924 \times 10^{-30} \text{ cm}^6 \text{ molecule}^{-2} \text{ s}^{-1}$$

(i)  $\langle \Delta E \rangle \propto T^{1/2}$  implies  $\langle \Delta E \rangle^{2055 \text{ K}} = 618 \text{ J mol}^{-1}$

$$\beta_c = 0.0267 \quad k_{\text{rec},0} = 1.58 \times 10^{-31} \text{ cm}^6 \text{ molecule}^{-2} \text{ s}^{-1}$$

$$n = 1.27$$

(ii)  $\langle \Delta E \rangle$  constant implies  $\langle \Delta E \rangle^{2055 \text{ K}} = 314 \text{ J mol}^{-1}$

$$\beta_c = 0.0143 \quad k_{\text{rec},0} = 8.45 \times 10^{-32} \text{ cm}^6 \text{ molecule}^{-2} \text{ s}^{-1}$$

$$n = 1.73$$

Table 1.—cont.

model B

$$k_{\text{rec},0}^{\text{sc}} = 1.37 \times 10^{-30} \text{ cm}^6 \text{ molecule}^{-2} \text{ s}^{-1}$$

(i)  $\langle \Delta E \rangle \propto T^{1/2}$  implies  $\langle \Delta E \rangle^{2055 \text{ K}} = 15100 \text{ J mol}^{-1}$ 

$$\beta_c = 0.348 \quad k_{\text{rec},0} = 4.78 \times 10^{-31} \text{ cm}^6 \text{ molecule}^{-2} \text{ s}^{-1}$$

$$n = 0.451$$

(ii)  $\langle \Delta E \rangle$  constant implies  $\langle \Delta E \rangle^{2055 \text{ K}} = 7702 \text{ J mol}^{-1}$ 

$$\beta_c = 0.226 \quad k_{\text{rec},0} = 3.10 \times 10^{-31} \text{ cm}^6 \text{ molecule}^{-2} \text{ s}^{-1}$$

$$n = 0.769$$

of weak-collision effects: most empirically derived collision efficiencies for He near room temperature are  $>0.1$  and usually  $<0.4$ .<sup>37,39</sup> Trøe<sup>21</sup> postulates that unusually low collision efficiencies may be due to the disappearance of some oscillators during a simple bond fission, being transformed into free rotors. Indeed, model B gives a value of  $\beta_c$  of 0.5, which is perhaps slightly higher than that often observed but which we consider a much better model of the present system. Further evidence arises from extrapolation to flame temperatures. The extrapolation depends on the nature of the temperature dependence of  $\langle \Delta E \rangle$ . There is a body of empirical evidence<sup>37,39</sup> indicating that  $\langle \Delta E \rangle$  varies as  $T^{1/2}$  in the case of He. For most other third bodies  $\langle \Delta E \rangle$  is found to be roughly independent of  $T$ . We have performed the extrapolation for both these cases for models A and B to the temperature of most of the test flames in the work of Jensen *et al.*<sup>16</sup>, *i.e.* 2055 K. The results are also listed in table 1. The extrapolations have also been fitted to expressions of the type  $k(T) = AT^{-n}$  and the values of  $n$  in each case are listed.

It was shown earlier that the fitted rate constant from the work of Jensen *et al.*<sup>16</sup> could be adjusted for He as a third body in place of the flame mixture. The estimated rate constant  $k_3(\text{K} + \text{OH} + \text{He}, T = 2055 \text{ K}) = 5.1 \times 10^{-31} \text{ cm}^6 \text{ molecule}^{-2} \text{ s}^{-1}$  is much closer to the extrapolated value from the present work using model B with  $\langle \Delta E \rangle \propto T^{1/2}$  than extrapolations using model A. Even the lower limit of the rate constant from Jensen's flame measurements of  $1.8 \times 10^{-31} \text{ cm}^6 \text{ molecule}^{-2} \text{ s}^{-1}$  is greater than the range predicted from model A. We therefore suggest that model B is a closer representation of the nature of the highly excited dissociating KOH.

Clearly, in proposing a value of  $n$  in a fitted extrapolation of the form  $T^{-n}$ , consideration must be given to the estimation of errors arising from the input data in the calculations. We have shown that the quoted errors in  $E_0$ , the frequencies of the oscillators and the estimation of the Lennard-Jones collision frequency are unlikely to give rise to errors in  $n$  of  $>\pm 10\%$ . The greatest source of uncertainty to which the calculation is most sensitive lies in the nature of the temperature dependence of  $\langle \Delta E \rangle$ . This is illustrated in table 1 for the two cases of  $\langle \Delta E \rangle \propto T^{1/2}$  or one which is independent of  $T$ , giving rise to a spread of  $n = 0.45\text{--}0.77$ . We would therefore recommend a value of  $n = 0.45$  with error limits of  $-0.05$  and  $+0.35$ .

The temperature dependence of  $k_3$  is thus concluded as

$$k_3(\text{K} + \text{OH} + \text{He}, 500 < T/\text{K} < 2100) = 1.48 \times 10^{-29} T^{-0.45 \pm 0.35} \text{ cm}^6 \text{ molecule}^{-2} \text{ s}^{-1}.$$

The rate constant for the reaction at 530 K from the present work was used to estimate a rate constant of  $4.1 \times 10^{-30} \text{ cm}^6 \text{ molecule}^{-2} \text{ s}^{-1}$  in a mixture of  $\text{H}_2 + \text{N}_2 +$

$H_2O$  at 530 K (see above). This can be used, together with the work of Jensen *et al.*<sup>16</sup> at 2055 K, to obtain the temperature dependence of the reaction as

$$k_3[K + OH + (H_2 + N_2 + H_2O), 500 < T/K < 2100] \\ = 1.28 \times 10^{-26} T^{-1.28} \text{ cm}^6 \text{ molecule}^{-2} \text{ s}^{-1}.$$

There are obviously rather large uncertainties in this extrapolation, but it nevertheless illustrates a higher temperature dependence than the empirically employed<sup>15</sup> use of  $T^{-1}$ .

In conclusion, apart from the description of the first direct measurement of  $k_3$ , the detailed extrapolation to flame temperatures and compositions described here shows good agreement between the present result and that derived from modelling on flames. This is an important general conclusion for the use of flame measurements, which normally involve sets of high-temperature equilibria for the determination of absolute rate data for reactions of the present type.

We thank the Ministry of Defence for an equipment grant. We are indebted to St John's College, Cambridge for a Research Fellowship held by J.M.C.P. during the tenure of which this work was carried out. C.C.X. thanks the Royal Society of London and the People's Republic of China for a Visiting Scholarship and the University of Science and Technology, Hefei, Anhui Province, for leave of absence during the period of which this work was performed. We finally thank Dr D. E. Jensen and Dr G. A. Jones of the Propellants, Explosives and Rocket Motor Establishment, Westcott for encouragement and helpful discussions.

<sup>1</sup> F. Kaufman, *Can. J. Chem.*, 1969, **47**, 1917.

<sup>2</sup> W. E. Kaskan, *10th Int. Symp. Combustion* (The Combustion Institute, Pittsburgh, U.S.A., 1965), p. 41.

<sup>3</sup> R. E. Carabetta and W. E. Kaskan, *J. Phys. Chem.*, 1968, **72**, 2483.

<sup>4</sup> D. Husain and J. M. C. Plane, *J. Chem. Soc., Faraday Trans. 2*, 1982, **78**, 163.

<sup>5</sup> D. Husain and J. M. C. Plane, *J. Chem. Soc., Faraday Trans. 2*, 1982, **78**, 1175.

<sup>6</sup> S. D. Kramer, B. E. Lehman, G. S. Hurst, M. G. Payne and J. P. Young, *J. Chem. Phys.*, 1982, **76**, 3014.

<sup>7</sup> L. W. Grossman, G. S. Hurst, S. D. Kramer, M. G. Payne and J. P. Young, *Chem. Phys. Lett.* 1977, **50**, 207.

<sup>8</sup> D. E. Jensen, *J. Chem. Soc., Faraday Trans. 1*, 1982, **78**, 2835.

<sup>9</sup> A. J. Hynes, M. Steinberg and K. Schofield, *J. Chem. Phys.*, 1984, **80**, 2385

<sup>10</sup> T. L. Brown, *Chem. Rev.*, 1973, **73**, 645.

<sup>11</sup> W. J. Baggaley, *Nature (London)*, 1975, **257**, 567.

<sup>12</sup> C. E. Kolb and J. B. Elgin, *Nature (London)*, 1976, **263**, 488.

<sup>13</sup> N. D. Sze, M. K. W. Ko, W. Swider and E. Murad, *Geophys. Res. Lett.* 1982, **9**, 1187.

<sup>14</sup> L. Thomas, M. C. Isherwood and M. R. Bowman, *J. Atmos. Terr. Phys.*, **45**, 587.

<sup>15</sup> D. E. Jensen and G. A. Jones, *Combust. and Flame*, 1978, **32**, 1.

<sup>16</sup> D. E. Jensen, G. A. Jones and A. C. H. Mace, *J. Chem. Soc., Faraday Trans. 1*, 1979, **75**, 2377.

<sup>17</sup> D. E. Jensen and G. A. Jones, *J. Chem. Soc., Faraday Trans. 1*, 1982, **78**, 2843.

<sup>18</sup> M. J. Howard and I. W. M. Smith, *Prog. React. Kinet.*, 1983, **12**, 55.

<sup>19</sup> P. W. Fairchild, G. P. Smith and D. R. Crosley, *J. Chem. Phys.*, 1983, **79**, 1795.

<sup>20</sup> J. Trøe, *J. Chem. Phys.*, 1977, **66**, 4745.

<sup>21</sup> J. Trøe, *J. Chem. Phys.*, 1977, **66**, 4758.

<sup>22</sup> C. R. Vidal and J. Cooper, *J. Appl. Phys.*, 1969, **40**, 3370.

<sup>23</sup> D. Husain, J. M. C. Plane and Chen Cong Xiang, *J. Chem. Soc., Faraday Trans. 2*, 1984, **80**, 713.

<sup>24</sup> P. K. Lengel and D. R. Crosley, *Chem. Phys. Lett.* 1974, **32**, 361.

<sup>25</sup> D. Husain, J. M. C. Plane and N. K. H. Slater, *J. Chem. Soc., Faraday Trans. 2*, **77**, 1949.

<sup>26</sup> *Atomic Energy Levels*, ed. C. E. Moore, *Natl Bur. Stand. U.S. Ref. Data Ser. no. 35* (U.S. Government Printing Office, Washington D.C., 1971), vol. I-III.

<sup>27</sup> *JANAF Thermochemical Tables*, project directors D. R. Stull and H. Prophet, *Natl Bur. Stand. U.S. NSRDS-NBS 37* (U.S. Government Printing Office, Washington D.C., 2nd edn, 1971).

- <sup>28</sup> W. Felder, A. Fontijn, H. N. Voltrauer and D. R. Voorhees, *Rev. Sci. Instrum.*, 1980, **51**, 195.
- <sup>29</sup> Yu. N. Novikov and M. E. Volpin, *Russ. Chem. Rev.*, 1971, **40**, 733.
- <sup>30</sup> I. P. Vonogradov and F. I. Vilesov, *Opt. Spectrosc.*, 1979, **44**, 653.
- <sup>31</sup> K. Schofield, *J. Phys. Chem. Ref. Data*, 1979, **8**, 723.
- <sup>32</sup> M. J. D. Powell, personal communication quoted in D. Husain and N. K. H. Slater, *J. Chem. Soc., Faraday Trans. 2*, 1980, **76**, 606.
- <sup>33</sup> K. P. Huber and G. Herzberg, *Molecular Spectra and Molecular Structure, IV Constants of Diatomic Molecules* (Van Nostrand Reinhold, New York, 1979).
- <sup>34</sup> R. Patrick and D. M. Golden, *Int. J. Chem. Kinet.* 1983, **15**, 1189.
- <sup>35</sup> R. B. Bird, W. E. Stewart and E. N. Lightfoot, *Transport Phenomena* (Wiley, New York, 1960).
- <sup>36</sup> R. Grice and D. R. Herschbach, *Mol. Phys.*, 1974, **27**, 159.
- <sup>37</sup> H. Endo, K. Glänzer and J. Tröe, *J. Phys. Chem.*, 1979, **83**, 2083.
- <sup>38</sup> S. H. Luu and J. Tröe, *Ber. Bunsenges. Phys. Chem.*, 1975, **77**, 325.
- <sup>39</sup> H. van den Burgh, N. Benoit-Guyot and J. Tröe, *Int. J. Chem. Kinet.* 1977, **9**, 223.
- <sup>40</sup> D. L. Baulch, R. A. Cox, R. G. Hampson, J. A. Kerr, J. Tröe and R. T. Watson, *J. Phys. Chem. Ref. Data* 1980, **9**, 295.
- <sup>41</sup> W. B. England, *J. Chem. Phys.*, 1978, **68**, 4896.
- <sup>42</sup> R. C. Reid, J. M. Prausnitz and T. K. Sherwood, *The Properties of Gases and Liquids* (McGraw-Hill, London, 1977), p. 400.
- <sup>43</sup> *JANAF Thermochemical Tables, J. Phys. Chem. Ref. Data, Suppl.*, 1974, **3**, 311.
- <sup>44</sup> G. J. Janz and R. P. Tomkins, *J. Phys. Chem. Ref. Data*, 1983, **12**, 591.
- <sup>45</sup> P. Kuijpers, T. Töring and A. Dymanus, *Z. Naturforsch., Teil A*, 1975, **30**, 1256.
- <sup>46</sup> D. E. Jensen, *J. Phys. Chem.*, 1970, **74**, 207.
- <sup>47</sup> J. T. Yardley, *Introduction to Molecular Energy Transfer* (Academic Press, London, 1980), pp. 125–127.
- <sup>48</sup> H. S. Johnston, *Gas Phase Reaction Rate Theory*, (The Ronald Press, New York, 1966), p. 286.

(PAPER 4/492)